ACS APPLIED MATERIALS & INTERFACES

RESEARCH ARTICLE

www.acsami.org

Multifunctional Gold–Silica Nanostructures for Ultrasensitive Electrochemical Immunoassay of Streptomycin Residues

Bingqian Liu, Bing Zhang, Yuling Cui, Huafeng Chen, Zhuangqiang Gao, and Dianping Tang*

Key Laboratory of Analysis and Detection for Food Safety (Ministry of Education & Fujian Province), Department of Chemistry, Fuzhou University, Fuzhou 350108, China

ABSTRACT: A facile and simple electrochemical immunoassay for ultrasensitive determination of streptomycin residues (STR) in food was designed by using nanogold-assembled mesoporous silica (GMSNs) as bionanolabels on a three-dimensional redox-active organosilica-functionalized sensing interface. To construct such a sensing interface, we initially synthesized organosilica colloids by using wet chemical method, and then utilized the prepared colloidal organosilica nanocomposites for the immobilization of monoclonal anti-STR antibodies on a glassy carbon electrode based on a sol–gel method. The bionanolabels were prepared based on coimmobilization of horseradish peroxidase (HRP) and STR-bovine serum albumin conjugates (STR-BSA) on the GMSNs. With a competitive-type immunoassay format, the assay toward STR analyte was carried out in pH 5.5 acetate acid buffer (ABS) by using redox-active organosilica nanocomposites as electron mediators, biofunctionalized GMSNs as traces, and hydrogen peroxide (H_2O_2) as enzyme substrate. Under optimal conditions, the reduction current of the electrochemical immunosensor decreased with the increase in STR level in the sample, and displayed a wide dynamic range of 0.05–50 ng mL^{-1} with a low detection limit (LOD) of 5 pg mL^{-1} at $3s_B$. Intra- and interassay coefficients of variation were less than 8.7 and 9.3% for STR detection, respectively. In addition, the methodology was validated with STR spiked samples including honey, milk, kidney, and muscle, receiving a good correspondence with the results obtained from high-performance liquid chromatography (HPLC).

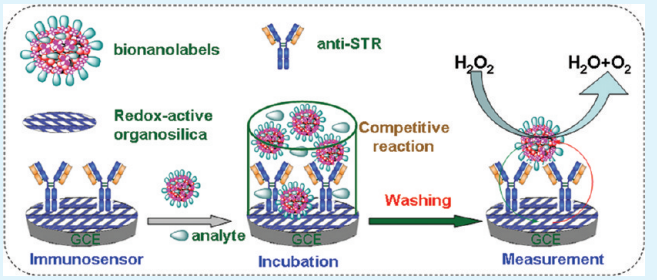

KEYWORDS: electrochemical immunoassay, food, streptomycin residues, immune-biosensor

1. INTRODUCTION

Streptomycin (STR), an aminoglycoside antibiotic, is used as a veterinary drug for the treatment of bacterial diseases.[1] Usually, it can inhibit both Gram-positive and Gram-negative bacteria, leading to codon misreading, eventual inhibition of protein synthesis and ultimately death of microbial cells, thus represents a useful broad-spectrum antibiotic.[2] Importantly, STR is also used as a pesticide to combat the growth of bacteria, fungi, and algae, and controls bacterial and fungal diseases of certain fruit, vegetables, seed, and ornamental crops, and controls algae in ornamental ponds and aquaria.[3] A major use is in the control of fireblight on apple and pear trees. Therefore, STR residues can be often found in food, such as meat, liver, kidney, milk and above all in honey. Although STR residues in food have none direct toxic effect, numerous allergic hypersensitivity cases were discovered in the recent years, and STR can induce severe skin rashes.[4] This has prompted adoption of regulatory limits in several countries, which, in turn, requires the development of validated official analytical methods for rapid and cost-effective screening of STR residues in food on a large scale.

Recently, various methods and strategies have been applied for the detection of STR residues in food, such as enzyme-linked immunoassay, chemiluminescence immunoassay, fluorescence immunoassay, and liquid chromatography.[5−9] The Baxter group fabricated an optical immunobiosensor for detection of STR residues in whole milk.[10] Knecht and co-workers designed a parallel affinity sensor array for the rapid automated analysis of 10 antibiotics in milk by using multianalyte immunoassays with an indirect competitive ELISA format.[11] Raz and his colleague constructed an imaging surface plasmon resonance-based immunosensor for label-free and multiplex detection of antibiotic residues in milk.[12] Despite many advances in this field, it is still a challenge to explore new approaches and strategies for the improvement of the sensitivity, simplification and feasibility of the detection method, especially at low concentration in food. Electrochemistry holds great potential as the next-generation detection strategy due to its high sensitivity, simple instrumentation, and excellent compatibility with miniaturization technologies.[13] However, to the best of our knowledge, there is almost no reports focusing on the electrochemical immunoassay for the detection of STR residues in food.[14]

Typically, the analytical properties of electrochemical immunoassays heavily depend on the signal-transduction method. High sensitivity is usually achieved by using an indicator system that results in the amplification of the measured product, such as enzyme labels or nanolabels. The Zhang group fabricated a new electrochemical immunosensor for the detection of microcystin-LR by

Received: August 13, 2011
Accepted: November 7, 2011
Published: November 07, 2011

using carbon nanotube and bioactive enzyme as labels.[15] Lai and his colleagues designed a dual signal amplification of glucose oxidase-functionalized nanocomposites as trace label for ultrasensitive simultaneous multiplexed electrochemical detection of tumor markers.[16] Recently, our group also fabricated various electrochemical immunoassays for the determination of biomarkers or biocompounds by coupling with enzyme labels and nanolabels, such as magnetic nanogold microspheres,[17] nanogold hollow microspheres,[18] enzyme-nanosilica-doped carbon nanotubes,[19] gold nanoparticle-decorated poly(amidoamine) dendrimer,[20] irregular-shaped gold nanoparticles,[21] and double-codified gold nanoparticles.[22] More significantly, we also recently found that mesoporous nanomaterials with large surface-to-volume ratios and uniform pore diameters were desirable especially for processes taking place at the phase boundary between solid particles and a liquid or gas phase as well as those relying on the flux of biomolecules or ions to and from active surfaces.[23−25] Moreover, the conductivity of mesoporous nanomaterials could be improved by doping noble metallic nanoparticles into the pores with an in situ synthesized method (e.g., nanogold or nanosilver particles), and the penetrated nanoparticles can serve as an intervening "spacer" matrix for electron communication.[26] In addition, mesoporous nanomaterials possess higher volume-to-surface ratio than that of solid nanoparticles, which can conjugate more biomolecule to improve the sensitivity of the assay.

Organosilica with good biocompatibility has received considerable attention due in large part to the potential for introducing a wide variety of structures into the backbone of the material via organic spacers of the monomer unit $[(R'O)_3Si\text{-}R\text{-}Si\text{-}(OR')_3]$.[27] Compared with conventional silica nanoparticles, organosilica can be prepared with high loadings of the functional group, distributed homogeneously throughout the bulk of material.[28,29] The accessible surface areas and density of organic groups are much larger than for grafted materials. Due to the ability to incorporate various organic compounds into the framework of silica materials there is a potential for the application of organosilica as solid catalysts and sensors. Some applications could benefit from a redox active framework. However, there are relatively very few examples of redox-active organosilica nanomaterials.[30,31] Herein, we synthesized redox-active organosilica nanostructures with three-dimensional network for the preparation of the electrochemical immunosensors, which were utilized for the determination of streptomycin residues in food by using nanogold-decorated mesoporous silica nanoparticles as bionanolabels for signal amplification of the immunoassay. With a competition-type immunoassay format, the formed immunocomplex was measured relative to the H_2O_2-ABS system. The aim of this work is to design a novel electrochemical immunoassay protocol for detection of ultralow-concentration STR in food.

2. EXPERIMENTAL SECTION

Rabbit antistreptomycin monoclonal antibody (anti-STR; Item number: STR-011A, 1.0 mg mL^{-1}) and streptomycin-bovine serum albumin conjugates (STR-BSA) were purchased from Beijing Biosynth. Biotechnol. Co. Ltd. (Beijing, China). Streptomycin standards (STR) with various concentrations were purchased from Beijing Dingguo Biotechnol. Co. Ltd. (Beijing, China). Tetraethoxysilane (TEOS), cetyltrimethylammonium bromide (CTAB), horseradish peroxidase (HRP), and thionine acetate salt (dye content ≥85%) were obtained from Sigma (USA). Poly(vinylpyrrolidone) (PVP, K-30), glucose, and $HAuCl_4 \cdot 4H_2O$ were purchased from Sinopharm Chem. Re. Co. Ltd. (Shanghai, China). Bovine serum albumin (BSA, 96−99%) was purchased from Shanghai Medpep Co. Ltd. (Shanghai, China). 3-(Methacryloyloxy) propyl trimethoxysilane and tertbuty hydroperoxide were purchased from Alfa Aesar. All reagents were of analytical grade and used as received without further purification. Ultrapure deionized water was generated using a Millipore Milli-Q plus system. 0.1 M acetic acid-buffered saline (ABS) with various pHs were prepared by mixing 0.1 M HAc and 0.1 M NaAc, and 0.1 M KCl was added as the supporting electrolyte. 0.1 M phosphate-buffered saline (PBS, pH 7.4) was prepared by adding 12.2 g K_2HPO_4, 1.36 g KH_2PO_4, and 8.5 g NaCl into 1000 mL of deionized water.

Electrochemical measurements were carried out with an Electrochemical Quartz Crystal Microbalance CHI 430A (China) with a conventional three-electrode system with a modified GCE as working electrode, a platinum foil as auxiliary electrode, and a saturated calomel electrode (SCE) as reference electrode. The sizes of nanomaterials were estimated from transmission electron microscopy (TEM) (H-7650, Hitachi Instrument, Japan). N_2 adsorption−desorption analysis was measured on a Micromeritics ASAP 2000 instrument (Micromeritics, Norcross, GA, USA). Pore volumes were determined using the adsorbed volume at a relative pressure of 0.99. Multipoint Brunauer−Emmet−Teller (BET) surface area was estimated from the relative pressure range from 0.06 to 0.3. The pore size distributions of the as-prepared samples were analyzed using the Barrett−Joyner−Halenda (BJH) method.

The three-dimensional redox-active organosilica nanostructures (TRSiNs) were synthesized according to the literature with some modification.[32] Prior to experiment, a stock solution of 0.5 wt % chitosan was prepared by adding 0.5 g of chitosan into 100 mL of acetic acid solution (1.0 wt %). Following that, the as-prepared chitosan suspension and 5 mL of thionine aqueous solution (3 mM) were injected into a flask equipped with a condenser, and vigorously stirred form 30 min under N_2 at room temperature (RT). Afterward, the solution was heated to 80 °C, and 2 mL of 3-(methacryloyloxy) propyl monomer was dropped into the mixture under stirring. After 20 min, 1 mL of tert-buty hydroperoxide (20 mM) aqueous solution was injected into the system. The mixture was further stirred for 4 h under N_2 until the stable latex was obtained. Finally, the three-dimensional redox-active organosilica nanostructures (designed as TRSiNs) were carefully washed and purified with 1.0 wt % acetic acid by centrifugation. The obtained TRSiNs were dispersed into 2 mL of pH 5.5 ABS ($C_{[TRSiN]} \approx 60$ mg mL^{-1}).

Mesoporous silica nanoparticles (MSNs) were synthesized according to the literature.[33] Briefly, 0.25 g of CTAB was initially dissolved in 120 mL of distilled water, and then 875 μL of sodium hydroxide (2.0 M) was injected into CTAB solution with stirring for 20 min at 80 °C. Afterward, 1.25 mL of TEOS was dropped into the above solution, and vigorously stirred for 2 h until white precipitates were obtained. Following that, the obtained product was filtered, washed with deionized water and methanol, and dried in air. Subsequently, 0.164 g of the precipitates was refluxed for 10 h in a mixture containing 1.5 mL of HCl (37%) and 75 mL of methanol to remove the surfactant template. The formed MSNs were filtered, washed with distilled water and methanol, and dried for 4 h at 60 °C.

Next, 10 mg of MSNs was initially dispersed in 10 mL of PVP aqueous solution (0.5 wt %), and then the mixture was vigorously stirring for 2 h at RT to make the positively charged PVP adsorb on the negatively charged MSNs. Afterward, the resulting mixture was centrifuged for 10 min at 12,000 g, and the obtained precipitate was redispersed in 4 mL of $HAuCl_4$ solution (1.0 wt %). The mixture was shaken slightly for 4 h at RT to make the $[AuCl_4]^-$ ions assemble on the surface of the PVP-functionalized MSNs. Subsequently, the Au(III) was reduced to zerovalent gold nanoparticles by using 0.2 M glucose solution at 95 °C. The obtained nanogold-assembled MSNs (designed as GMSNs) were collected by centrifugation, and dispersed into 1 mL of pH 9.0 Tris-buffer solution for the bioconjugation of STR-BSA and HRP.

Scheme 1. (a) Illustration of Fabrication Process of the Bionanolabels and (b) Measurement Protocol of the Competitive-Type Electrochemical Immunoassay for STR Sample in Food

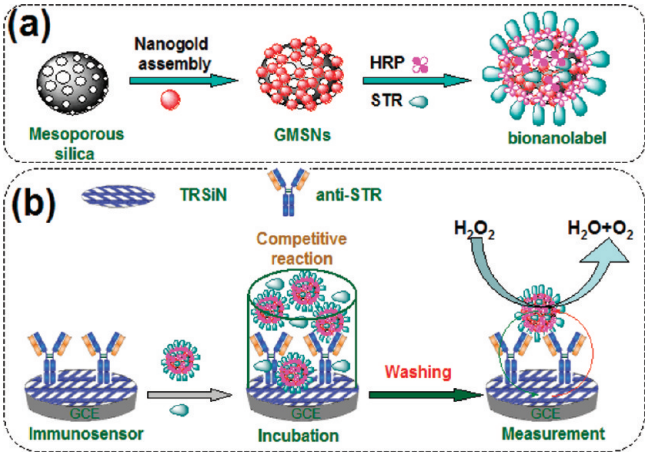

500 μL of STR-BSA conjugates (100 ng mL^{-1}) and 100 μL of HRP (1 mg L^{-1}) were initially injected into the prepared above GMSN solution, and the mixture was then incubated for 12 h at 4 °C with slightly shaking. The STR-BSA and HRP-labeled GMSNs (designed as bionanolabels) were collected by centrifugation for 10 min at 12,000 g at 4 °C. After washing and centrifugation, the resulting precipitates were redispersed in 1 mL of pH 7.4 PBS for further usage ($C_{[MSN]} \approx 10$ mg mL^{-1}).

Before modification, a glassy carbon electrode (GCE, 1 mm in diameter) was polished with 0.3 and 0.05 mm alumina, rinsed with distilled water, acetone and ethanol, and dried in air. The electrochemical immunosensor was fabricated by using a conventional sol−gel method. Initially, 5 μL of anti-STR (1.0 U mL^{-1}) was mixed with 30 μL of TRSiN colloids ($C_{[TRSiN]} \approx 60$ mg mL^{-1}) in a small beaker, and the mixture was then adequately stirred. Following that, 3 μL of the TRSiN-anti-STR colloids was thrown on the surface of the cleaned GCE, and dried at RT. To eliminate the nonspecific effect, we treated the modified electrode with 2.5 wt % BSA for 60 min at RT, followed by washing carefully 3 times with pH 7.4 PBS. The as-prepared immunosensors were stored at 4 °C when not in use.

Prior to measurement, an incubation solution was prepared by mixing 5 μL of different STR levels or samples and 5 μL of bionanolabels. During each run, the incubation solution was dropped on the electrochemical immunosensor and incubated for 30 min at RT (*Note*: this step should be conducted in a container to avoid the evaporation of incubation solution.). The electrochemical measurement was recorded in a pH 5.5 ABS containing 1.0 mM H_2O_2. The detection solution was bubbled thoroughly with high purity nitrogen for 10 min and maintained under nitrogen. The differential pulse voltammetric (DPV) measurements were from −200 to −500 mV with pulse amplitude of 50 mV and width of 20 ms. The DPV peak current regarded as the signal of the immunosensor was relevant to the concentration of STR. Analyses are always made in triplicate. All measurements were carried out at RT (25 ± 1.0 °C). The measurement protocol is shown in Scheme 1. After each immunoassay run, the immunosensors were regenerated by immersing into 0.2 M glycine-HCl (pH 2.8) for 5 min, washing with pH 7.4 PBS, and then carrying out the following run cycle.

Honey, peanut, and milk were purchased from a local supermarket. Porcine kidney and muscle samples were purchased from Fujian Food and Drug Division. These samples were assayed using the electrochemical immunoassay after incubation with matrix-STR for 30 min.

Calibration Curve. The calibration curve of the electrochemical immunoassay was calculated by spiking STR standards into the blank peanut samples according to our previous report.[34] Prior to the experiment, peanut standards were prepared as follows: 5.0 g of ground blank peanut samples were extracted with 37.5 mL of MeOH/water (80:20, v/v) with stirring for 1 h and followed by filtration. The extract (20 mL) was diluted into 60 mL of H_2O. Finally, standard samples were prepared by spiking aliquots of STR standards into different volumes of diluted extract.

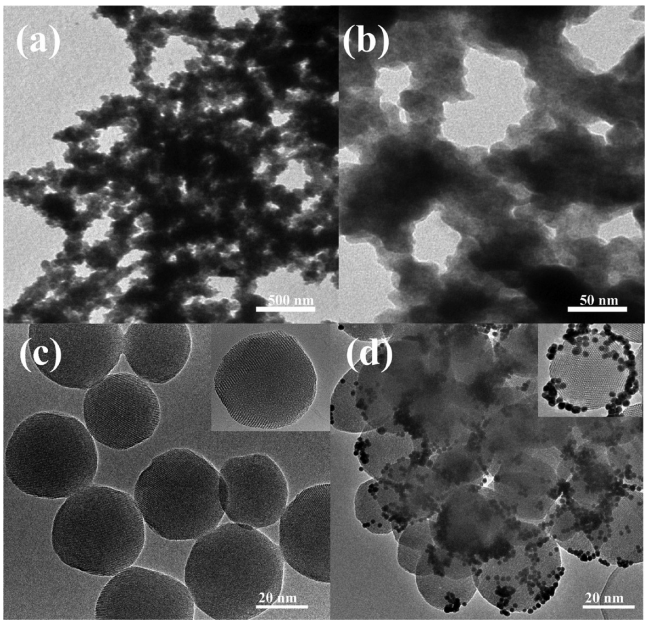

Figure 1. TEM images of (a) the prepared TRSiNs, (b) image a with high amplification, (c) the MSNs, and (d) the GMSNs (inset: high-magnification images).

Honey, Milk, Porcine Kidney, and Muscle Sample Spiking. The spiking process was similar to that in our recent report.[19] Briefly, 15 mL samples including honey and milk were initially transferred directly into a centrifuge tube, respectively, and these samples were then centrifuged for 20 min at 13 000 g. The resulting suspension was transferred into a fresh tube at a finite volume of 15 mL with distilled water. For the porcine kidney and muscle samples, 3.75 g of sample was initially placed in a centrifuge tube, and then 15 mL of methanol/water (80:20, v/v) was added, and the mixtures were then sonicated for 60 s to assist extraction. Following that, these samples were centrifuged for 20 min at 13 000 g. Finally, 3 mL of the suspension was collected and transferred into another centrifuge tube and diluted to 15 mL with distilled water. The real samples were prepared by spiking aliquots of STR standards into different volumes of extraction. These spiking food samples were measured by using the electrochemical immunoassay.

3. RESULTS AND DISCUSSION

In general, a bionanocomposite is formed by combination with two or more phases of different natures. The formed bionanocomposite acts not only as a support for the immunologic material but also a transducer. The binding material is essential in the formation of the bionanocomposites. In this study, we synthesized three-dimensional redox-active organosilica colloids for the construction of the immunosensing interface. Use of the TRSiNs is expected to enhance the immobilized amount of biomolecules due to the unique physical and chemical features of three-dimensional nanostructures. Meanwhile, the redox-active thionine molecules, as the mediators of the electron transfer were encapsulated in the organosilica nanostructures, which facilitated the electrochemical monitoring of the immunosensors.

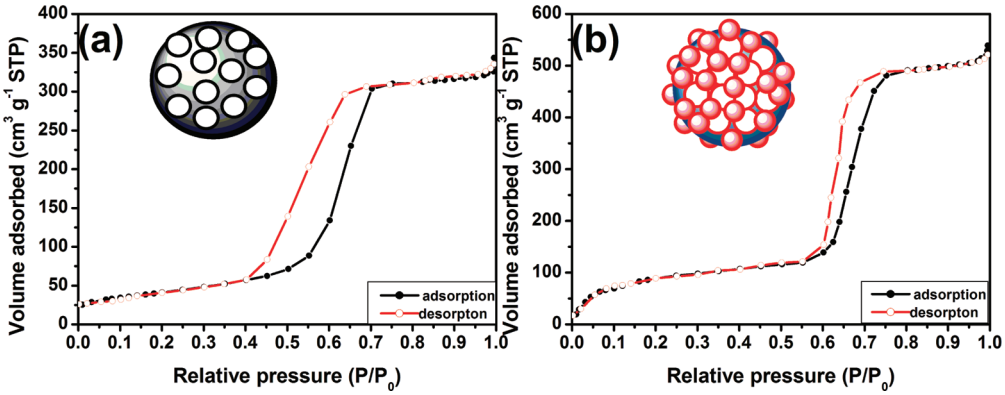

Figure 2. N_2 adsorption−desorption isotherms of (a) MSNs and (b) GMSNs at 77 K.

Figure 1a shows the transmission electron microscope (TEM) image of the synthesized TRSiNs. As seen from Figure 1b, the organosilica colloids exhibited three-dimensional network, and the frameworks were composed of high silica nanoparticles. The formation of the network could not only facilitate the conjugation of biomolecules, but also favor for the electron communication between the solution and the base electrode through the interspace.

For the development of the competitive-type electrochemical immunoassay, the preparation of the bionanolabels was crucial. Herein, the STR-BSA and HRP were labeled on the surface of the GMSNs through the strong interaction between gold nanoparticles and proteins. Therefore, the successful synthesis of GMSNs is a precondition. Figure 1c displays the TEM image of the as-synthesized MSNs, and the mean size was about 100 nm. Significantly, it can be seen that many small pores were penetrated into or coated on the silica nanostructures. At this condition, $[AuCl_4]^-$ ions could be immobilized outside and inside of the MSNs by using PVP as cross-linkage reagent. As seen from Figure 1d, a large number of gold nanoparticles could be achieved on the MSNs after $[AuCl_4]^-$ ions were in situ reduced to zerovalent Au^0 by glucose. The appearance of gold nanoparticles provided a biocompatible interface and a good microenvironment for the conjugation of STR-BSA and HRP.

The N_2 adsorption−desorption isotherm of mesoporous silica nanoparticles before the incorporation of a gold source was type IV with an H1 hysteresis loop, which is typically observed for mesoporous materials (Figure 2a). The BET (Brunauer, Emmet, Teller) surface area of the synthesized MSNs was about 532.8 $m^2\ g^{-1}$, which was calculated by employing the Broekhoff-de Boer equation with the D−H algorithm using a cylindrical pore model. The N_2 adsorption−desorption isotherm of the as-prepared GMSNs was also type IV with an H1 hysteresis loop as with pure MSNs, and the BET surface area decreased to 297.1 $m^2\ g^{-1}$ (Figure 2b). Moreover, the synthesized GMSNs exhibited a two-step desorption isotherm in a relative pressure range of 0.5 to 0.8. This was related to the pore blocking effect. Desorption of nitrogen molecules was impeded by the presence of gold nanoparticles in the mesoporous silica nanoparticles.

Figure 3 shows the cyclic voltammograms of variously modified electrode at 50 mV s^{-1} in pH 5.5 ABS. No redox peaks were observed at the bare GCE (Figure 3a). When the anti-STR-doped TRSiNs were modified onto the surface of the GCE, a couple of redox peaks at −0.5 mV and 0.2 mV were achieved (Figure 3b). The peaks mainly derived from the doped thionine in the organosilica nanostructures according to our previous experiment.[35] The results indicated that the redox properties of the thionine, a good electron mediator, were not changed when it was encapsulated in the organosilica nanostructures. To monitor the stability of the electrochemical immunosensor, the GCEs coated with anti-STR and TRSiNs were stored into pH 7.4 PBS, and measured periodically by cyclic voltammetry. Alternatively, the anti-STR-TRSiNs-modified GCEs were stored dry at 4 °C over pH 7.4 PBS for most of the storing time, and cyclic voltammograms were run occasionally after returning the dry electrodes to buffer solutions. For both storage conditions, the peak currents of the modified electrodes decreased 98.9, 97.7, 96.3, and 95.1% of the initial currents at 5th, 10th, 15th, and 20th day (n = 3), respectively. The results indicated that thionine and anti-STR molecules could be firmly immobilized on the GCE electrode through the synthesized organosilica network.

To investigate the feasibility of the competitive-type electrochemical immunoassay, we utilized the as-prepared immunosensor for the determination of two STR levels including 0 ng mL^{-1} and 10 ng mL^{-1} STR (as examples). Initially, we monitored the electrochemical characteristic of the as-prepared immunosensor toward zero analyte in pH 5.5 ABS at the absence (Figure 3c) and presence (Figure 3d) of 1.0 mM H_2O_2. Because of the absence of STR analyte in the incubation solution, the immobilized anti-STR on the electrode adequately reacted with the STR labeled on the bionanolabels. The formed immunocomplex could act as an inert layer, and hindered the electron transfer (Figure 3c). So, the peak current decreased in comparison with that of Figure 3b. However, upon addition of 1.0 mM H_2O_2 in pH 5.5 ABS, an obvious redox reaction was observed with a distinct increase of the reduction current and a decrease of the oxidation current (Figure 3d). The increase in the cathodic current mainly originated from the labeled HRP on the bionanolabels toward the catalytic reduction of H_2O_2 with the aid of thionine. Significantly, the cathodic current decreased with the increment of STR concentration in the incubation solution (Figure 3e). Therefore, we might quantitatively evaluate the level of STR in the sample according to the change in the cathodic currents. The reaction process and measurement principle of the electrochemical immunoassay could be schematically explained as follows:

Immunoreaction process:

$$\text{anti-STR(electrode)} + (\text{bionanolabel} + \text{STR}) \rightarrow \text{anti-STR-bionanolabel} \quad (1)$$

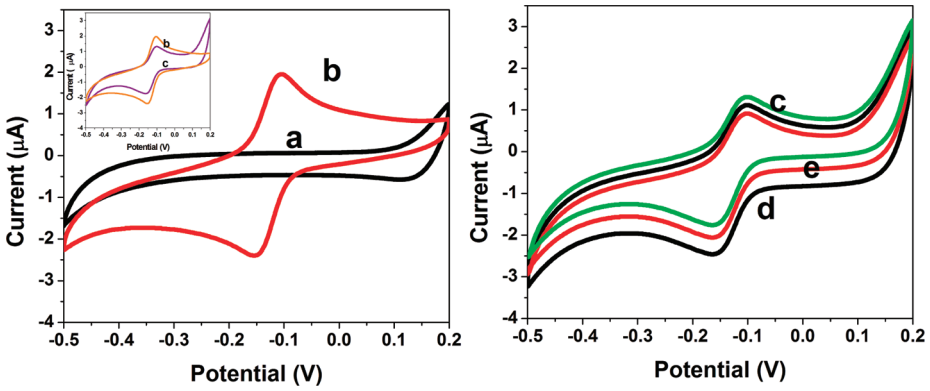

Figure 3. Cyclic voltammograms of (a) GCE in pH 5.5 ABS, (b) anti-STR-TRSiN/GCE in pH 5.5 ABS, (c) electrode from b after incubation with 0 ng mL^{-1} STR and excess bionanlabels in pH 5.5 ABS, (d) electrode from c in pH 5.5 ABS containing 1.0 mM H_2O_2, and (e) electrode from b after incubation with 10 ng mL^{-1} STR and excess bionanlabels in pH 5.5 ABS containing 1.0 mM H_2O_2; scan rate: 50 mV s^{-1}.

Electrochemical measurement:

$$HRP_{(red)} + H_2O_2 \rightarrow HRP_{(ox)} + H_2O \quad (2)$$

$$HRP_{(ox)} + \text{thionine}_{(red)} \rightarrow HRP_{(red)} + \text{thionine}_{(ox)} \quad (3)$$

$$\text{thionine}_{(ox)} + 2H^+ \rightarrow \text{thionine}_{(red)} \quad (4)$$

In an effort to evaluate the repeatable usability of the immunosensor, 0.1 M glycine−HCl solution (pH 2.8) was used to break the antibody−antigen linkage. After detecting 10 ng mL^{-1} STR, the immunosensor was dipped into the glycine−HCl solution for 5 min, and removed to detect 10 ng mL^{-1} STR again. The immunosensor retained 93.9% of the initial current after 5 regeneration cycles.

To further demonstrate the amplified properties of the as-synthesized bionanolabels toward the electrochemical signal of the immunoassay, we prepared five types of bionanolabels, i.e., HRP directly labeled with BSA-STR conjugates (HRP-STR), gold nanoparticle colabeled with HRP and STR (HRP-STR-AuNP, 16 nm in diameter for AuNPs), MSN colabeled with HRP and STR (HRP-STR-MSN, 100 nm in diameter for MSNs), solid silica-AuNP hybrid colabeled with HRP and STR (HRP-STR-GSN, 100 nm in diameter for solid silica nanoparticles) and GMSN colabeled with HRP and STR (HRP-STR-GMSN), which were used for determination of 10.0 ng mL^{-1} STR (as an sample) on the organosilic-functionalized immunosensor under the same conditions, respectively. The comparison was based on the shift in the cathodic current relative to zero analyte (i.e., 0 ng mL^{-1} STR). The results are listed in Figure 4. As seen from Figure 4, the shift in the cathodic current by using HRP-STR-GMSNs as signal tags were significantly larger than those of other bionanolabels. Some possible explanations may contribute to these observations: (i) the synthesized GMSNs can provide a large room for the immobilization of nanogold and biomolecules; (ii) gold nanoparticles are in situ synthesized on the MSNs or into the nanopores, which greatly improved the conductivity of the MSNs; and (iii) the presence of many STR-BSA molecules on the GMSNs can increase the possibility of antigen−antibody interaction. When one STR on the GMSNs reacts with one anti-STR on the electrode, the whole bionanolabel can participate in the electrochemical reaction.

To achieve an optimal electrochemical response of the immunoassay, we usually optimize the pH of the detection solution. Figure 5a shows the effect of the pH value of ABS on the cathodic current of the electrochemical immunoassay by using 10 ng mL^{-1} STR as an example. Initially, the as-prepared immunosensor was incubated for 60 min (*Note*: the aim was to ensure the adequate interaction of antigens and antibodies) at RT with the incubation solution containing 5 μL of 10 ng mL^{-1} STR and 5 μL of bionanolabels ($C_{[MSN]} \approx 10$ mg mL^{-1}). Then, the obtained immunosensors were monitored by voltammetry in HAc-NaAc buffer systems with various pH values containing 1.0 mM H_2O_2. The judgment was based on the cathodic current of the immunosensor. Experimental results indicated that the cathodic current showed a trend of first increase and then decrease with the increment of pH of ABS. However, an optimal current response was observed at pH 5.5 ABS. Considering the bioactivity and bioelectrocatalytic efficiency of these proteins, a compromise pH of 5.5 was chosen for the detection of STR.

In general, incubation time and incubation temperature for the antigen−antibody interaction often affect the analytical properties of the electrochemical immunoassay. However, considering the practical application of the electrochemical immunosensor, all experiments were carried out at RT (25 ± 1.0 °C). At this condition, various incubation times were investigated by using 10 ng mL^{-1} STR as an example. As seen from Figure 5b, the cathodic currents increased with the increase of incubation time, and tended to level off after 30 min. Longer incubation time did not significantly improve the response. Thus, 30 min was chosen for the antigen−antibody reaction.

Under optimal conditions, the sensitivity and dynamic range of the electrochemical immunoassay was investigated toward STR standards in pH 5.5 ABS containing 1.0 mM H_2O_2 by using HRP-STR-GMSNs as trace and H_2O_2 as enzyme substrate with a competitive-type immunoassay format. As indicated from the inset of Figure 6a, the DPV peak currents of the electrochemical immunoassay decreased with the increase of STR concentrations, and exhibited a linear relationship between the DPV peak currents and the STR concentration in the range from 0.05 to 50 ng mL^{-1}. The regression equation was $I\ (\mu A) = -1.6915 + 0.0291 \times C_{[STR]}$ (ng mL^{-1}, $R^2 = 0.9882$) (Figure 6b) with a detection limit (LOD) of 5 pg mL^{-1} STR at a signal-to-noise ratio of 3σ (where σ is the standard deviation of the blank, $n = 13$), which was obviously lower than those of immunochemical method (10 μg $kg^{-1} \approx 10$ ng mL^{-1}),[5] enzyme-linked immunoassay (1 ng mL^{-1}),[6] microplate-array based SMM-FIA (2.01 ng mL^{-1}),[9] optical immunobiosensor (4.1 ng mL^{-1}),[10] and liquid chromatography (8 μg $kg^{-1} \approx 8$ ng mL^{-1}).[36]

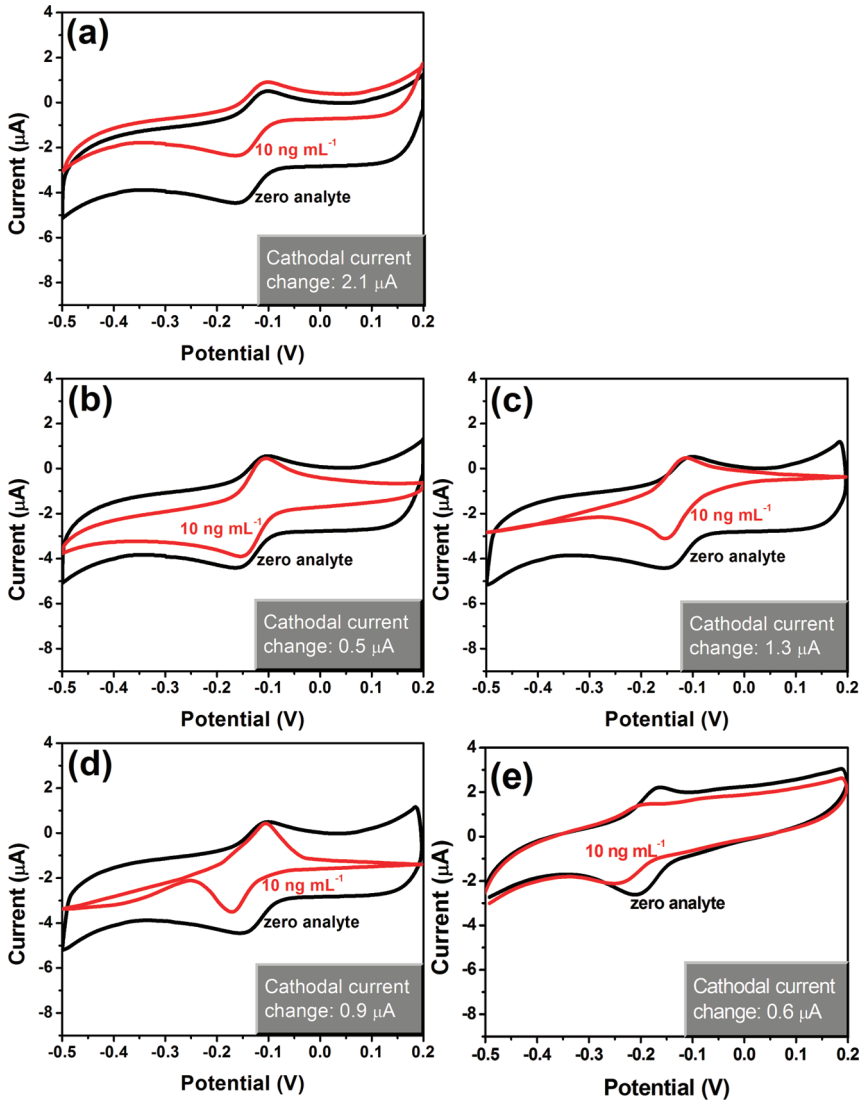

Figure 4. Comparison of electrochemical responses of the anti-STR-TRSiN/GCE by using various signal tags: (a) HRP-STR-GMSNs, (b) HRP-STR, (c) HRP-STR-AuNPs, (d) HRP-STR-MSNs, and (e) HRP-STR-GSNs toward 10 ng mL^{-1} STR (black line) relative to zero analyte (red line) in pH 5.5 ABS containing 1.0 mM H_2O_2.

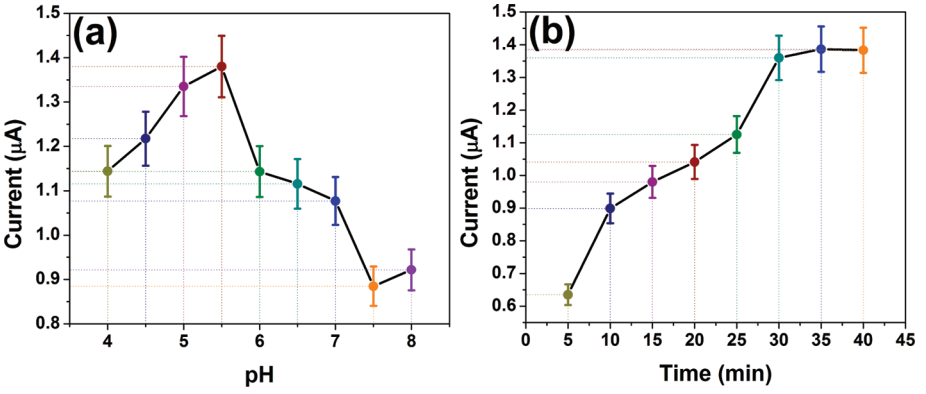

Figure 5. Effect of (a) pH of ABS and (b) incubation time on the electrochemical response of the immunoassay.

To investigate the reproducibility of the electrochemical immunoassay, we repeatedly assayed three levels of STR samples, using identical batches of immunosensors and bionanolabels throughout. Experimental results indicated that the coefficients

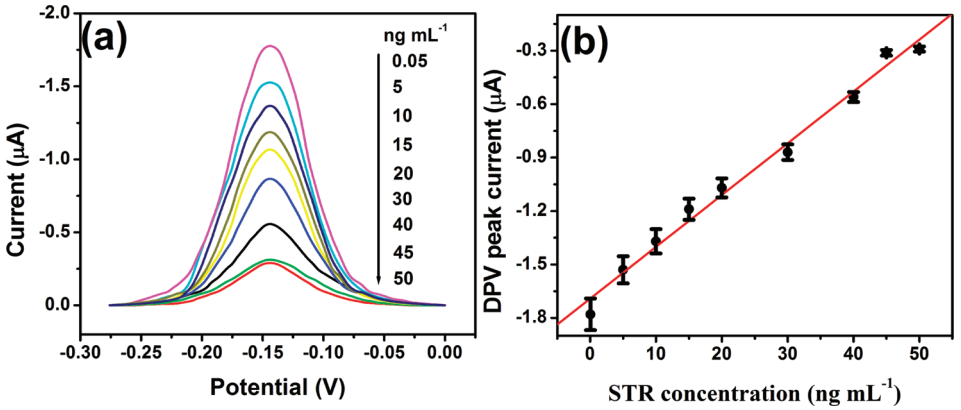

Figure 6. (a) DPV curve of the electrochemical immunoassay toward STR standards in pH 5.5 ABS containing 1.0 mM H_2O_2 and (b) calibration plots (Note: incubation time, 30 min; incubation temperature, RT).

Table 1. Interference Degree or Crossing Recognition Level of the Electrochemical Immunoassay

	$C_{[\text{interfering agents}]}$ (ng mL^{-1}); detectable concentration [b]						
substrate[a]	0	1.0	5.0	10.0	15.0	mean ± SD	RSD (%)
STR + AFB_1	10.0	10.08 ± 0.05	10.21 ± 0.11	10.35 ± 0.19	10.49 ± 0.47	10.23 ± 0.18	1.8
STR + AFB_2	10.0	10.19 ± 0.06	10.29 ± 0.73	10.57 ± 0.32	10.34 ± 0.98	10.50 ± 0.34	3.2
STR + DDSTR	10.0	10.61 ± 0.03	12.5 ± 0.23	16.6 ± 0.58	22.7 ± 0.51	14.48 ± 4.71	32.5
STR + SEB	10.0	10.15 ± 0.03	10.41 ± 0.78	10.87 ± 0.51	10.59 ± 0.88	10.40 ± 0.31	2.98
STR + DHSTR	10.0	10.74 ± 0.01	13.3 ± 0.86	16.1 ± 0.77	23.6 ± 0.38	14.75 ± 4.92	33.4
STR + IL-6	10.0	10.05 ± 0.01	10.68 ± 0.46	10.71 ± 0.91	10.93 ± 0.74	10.25 ± 0.21	2.05

[a] Containing 10 ng mL^{-1} STR and various concentrations of interfering agents. [b] The average value of three assays, and the concentrations were calculated according the calibration curve.

Table 2. Comparison of Determination Results for STR in Spiked Food Samples as Obtained by the Electrochemical Immunoassay and HPLC as Reference Method

			methods (mean ± SD, ng mL^{-1})[a] and recovery (%)	
food sample	sample no.	spiked STR (ng mL^{-1})	electrochemical immunoassay	HPLC
milk	1[b]	0	0.05 ± 0.03 (−)	[c]
	2	2.5	2.69 ± 0.23 (108%)	2.58 ± 0.11 (103%)
	3	5.0	5.31 ± 0.34 (106%)	5.72 ± 0.38 (114%)
	4	10.0	9.69 ± 0.78 (96.9%)	9.41 ± 0.25 (94.1%)
honey	5[b]	0	0.09 ± 0.03 (−-)	0.11 ± 0.02 (122.2%)
	6	2.5	2.38 ± 0.53 (95.2%)	2.67 ± 0.17 (107%)
	7	5.0	5.47 ± 0.31 (109%)	4.59 ± 0.68 (91.8%)
	8	10.0	10.76 ± 0.62 (108%)	10.83 ± 0.79 (108%)
kidney	9[b]	0	0.07 ± 0.01 (−)	[c]
	10	1.0	1.14 ± 0.46 (114%)	1.05 ± 0.27 (105%)
	11	3.5	3.91 ± 0.94 (112%)	3.38 ± 0.83 (96.6%)
	12	7.0	6.84 ± 1.08 (97.7%)	7.17 ± 0.57 (102%)
muscle	13[b]	0	[c]	[c]
	14	1.0	0.94 ± 0.34 (94.0%)	0.98 ± 0.42 (98.0%)
	15	3.5	3.70 ± 0.79 (106%)	3.86 ± 0.71 (110%)
	16	7.0	7.57 ± 0.19 (108%)	6.80 ± 0.19 (97.1%)

[a] Each sample was assayed in triplicate. [b] Without spiking STR samples. [c] Not detected.

of variation (CVs) of the intra-assay between six runs were 9.3, 6.1, and 4.7% for 0.5 ng mL^{-1}, 10 ng mL^{-1} and 30 ng mL^{-1} STR, respectively, whereas the CVs of the interassay with various batches were 7.9, 9.5, and 7.2% toward the above-mentioned analyte. The low CVs indicated that the electrochemical immunoassay could be used repeatedly, and further verified the possibility

of batch preparation. When the immunosensors and bionanolabels were not in use, they were stored at 4 °C. No obvious change was observed after storage for 15 days but a 10% decrease of its initial currents was noticed after 35 days.

To monitor the differences in response of the electrochemical immunoassay to interference degree of crossing recognition level, aflatoxin B_1 (AFB_1), aflatoxin B_2 (AFB_2), staphylococcal enterotoxin B (SEB), dihydrostreptomycin (DHSTR), dihydrodesoxystreptomycin (DDSTR), and interleukin-6 (IL-6) with various concentrations were injected into the incubation solution, respectively. The current responses to each-type analyte were recorded, and the results are listed in Table 1. As shown in Table 1, almost no response was observed toward AFB_1, AFB_2, SEB and IL-6, while there is a high cross-reactivity with DHSTR and DDSTR. The reason might be the fact that the monoclonal anti-STR antibodies have high cross reactivity with DHSTR and DDSTR of STR similar structure. Thus, the selectivity of the electrochemical immunoassay is acceptable.

To the possible application of the electrochemical immunoassay for testing real food samples, STR spiked samples, including milk, honey, kidney and muscle, were assessed by using the electrochemical immunoassay and HPLC as a reference method (finished by Drs. L. Xu and J. Liao, SWU, Chongqing). The experimental results are summarized in Table 2. The recovery in spiked samples is 94−114% for the electrochemical immunoassay. Comparison of the experimental results obtained with the proposed immunoassay with those of HPLC was also performed *via* the use of a least-squares regression method. The regression line was fitted to $y = 0.978\,x - 0.002$ ($R^2 = 0.982$) where x stands for the STR concentrations estimated with the electrochemical immunoassay and y stands for those of the HPLC. No significance differences were encountered between the optimum values of intercept and slope and experimental data, thereby revealing a good agreement between both analytical methods.

4. CONCLUSION

This manuscript describes an ultrasensitive electrochemical immunoassay for the detection of streptomycin residues in foodstuffs by using nanogold-assembled mesoporous silica nanostructures as bionanolabels on three-dimensional redox-active organosilica-functionalized sensing interface. The synthesized bionanolabels are proved to be an efficient signal amplifier because of the high pore volume and large surface area of the nanostructures. Experimental results indicated that the analytical properties of the electrochemical immunoassay could be improved with the aid of the GMSNs. The highlight of this work is to successfully fabricate an ultrasensitive electrochemical immunoassay based on a novel bionanolabel. This research could open new avenues in the application of mesoporous materials-based nanocables. Importantly, the electrochemical immunoassays can be further extended for detection of other low-concentration toxins in food by controlling the target antibody. We might suspect that such immunoassay approaches will evolve toward a very promising future for reliable point-of-care diagnostics of biocompounds.

AUTHOR INFORMATION

Corresponding Author

*Phone: +86 591 2286 6125. Fax: +86 591 2286 6135. E-mail: dianping.tang@fzu.edu.cn.

ACKNOWLEDGMENT

This work was supported by the National Natural Science Foundation of China (21075019, 41176079, 20735002), the Research Fund for the Doctoral Program of Higher Education of China (20103514120003), the Award Program for Minjiang Scholar Professorship for Returned High-Level Overseas Chinese Scholars (XRC-0929) and the "973" National Basic Research Program of China (2010CB732403). Drs. L. Xu and J. Liao (SWU, Chongqing) are thanked for HPLC analysis of real samples for the method-comparison study.

REFERENCES

(1) Sheth, H.; Yaylayan, V.; Low, N.; Stiles, M.; Sporns, P. *J. Agric. Food Chem.* **1990**, *38*, 1125–1130.
(2) Schatz, A.; Bugie, E.; Waksman, S. *Proc. Soc. Exp. Biol. Med.* **1944**, *55*, 66–69.
(3) Cazoto, L.; Martins, D.; Ribeiro, M.; Duran, N.; Nakazato, G. *J. Antibiot.* **2011**, *64*, 395–397.
(4) Que, Y.; Moreillon, P. *Nat. Rev. Cardiol.* **2001**, *8*, 322–326.
(5) Heering, W.; Usleber, E.; Dietrich, R.; Märtlbauer, E. *Analyst* **1998**, *123*, 2759–2762.
(6) Ramadan, A.; Abuknesha.; Luk, C. *Analyst* **2005**, *130*, 964–970.
(7) Edder, P.; Cominoli, A.; Corvi, C. *J. Chromatogr., A* **1999**, *830*, 345–351.
(8) Ferguson, J.; Baxter, G.; McEvoy, J.; Stead, S.; Rawlings, E.; Sharman, M. *Analyst* **2002**, *127*, 951–956.
(9) Ye, B.; Li, S.; Zuo, P.; Li, X. *Food Chem.* **2008**, *106*, 797–803.
(10) Baxter, G.; Ferguson, J.; O'Connor, M.; Elliott, C. *J. Agric. Food Chem.* **2001**, *49*, 3204–3207.
(11) Knecht, B.; Strasser, A.; Dietrich, R.; Martlbauer, E.; Niessner, R.; Weller, M. *Anal. Chem.* **2004**, *76*, 646–654.
(12) Raz, S.; Bremer, M.; Haasnoot, W.; Norde, W. *Anal. Chem.* **2009**, *81*, 7743–7749.
(13) Tang, D.; Zhong, Z.; Niessner, R.; Knopp, D. *Analyst* **2009**, *134*, 1554–1560.
(14) Wei, Z.; Wang, J. *Anal. Chim. Acta* **2011**, *694*, 46–56.
(15) Zhang, J.; Lei, J.; Xu, C.; Ding, L.; Ju, H. *Anal. Chem.* **2010**, *82*, 1117–1122.
(16) Lai, G.; Yan, F.; Ju, H. *Anal. Chem.* **2009**, *81*, 9730–9736.
(17) Tang, D.; Yuan, R.; Chai, Y. *Anal. Chem.* **2008**, *80*, 1582–1588.
(18) Tang, D.; Ren, J. *Anal. Chem.* **2008**, *80*, 8064–8070.
(19) Tang, D.; Tang, J.; Su, B.; Chen, G. *J. Agric. Food Chem.* **2010**, *58*, 10824–10830.
(20) Tang, D.; Tang, J.; Su, B.; Huang, J.; Qiu, B.; Chen, G. *Biosens. Bioelectron.* **2010**, *26*, 3219–3226.
(21) Tang, J.; Su, B.; Tang, D.; Chen, G. *Biosens. Bioelectron.* **2010**, *25*, 2657–2662.
(22) Tang, D.; Su, B.; Tang, J.; Ren, J.; Chen, G. *Anal. Chem.* **2010**, *82*, 1527–1534.
(23) Li, Q.; Tang, D.; Tang, J.; Su, B.; Chen, G.; Wei., M. *Biosens. Bioelectron.* **2011**, *27*, 153–159.
(24) Tang, J.; Tang, D.; Niessner, R.; Chen, G.; Knopp, D. *Anal. Chem.* **2011**, *83*, 5407–5414.
(25) Li, Q.; Zeng, L.; Wang, J.; Tang, D.; Liu, B.; Chen, G.; Wei, M. *ACS Appl. Mater. Interfaces* **2011**, *3*, 1366–1373.
(26) Martins, J.; Batista, R.; Chacham, H. *J. Am. Chem. Soc.* **2010**, *132*, 11929–11933.
(27) Xia, Y.; Yang, Z.; Mokaya, R. *J. Chromatogr., A* **2007**, *1149*, 219–227.
(28) Xia, Y.; Yang, Z.; Mokaya, R. *Chem. Mater.* **2006**, *18*, 1141–1148.
(29) Melero, J.; Grieken, R.; Morales, G. *Chem. Rev.* **2006**, *106*, 3790–3812.
(30) Walcarius, A.; Mandler, D.; Cox, J.; Collinson, M.; Lev, O. *J. Mater. Chem.* **2005**, *15*, 3663–3689.
(31) alkus, K., Jr.; Pisklak, T.; Hundt, G.; Sibert, J.; Zhang, Y. *Microporous Mesoporous Mater.* **2008**, *112*, 1–13.

(32) Fei, B.; Lu, H.; Xin, J. *Polymer* **2006**, *47*, 947–950.
(33) Lai, C.; Trewyn, B.; Jeftinija, D.; Jeftinija, K.; Xu, S.; Jeftinija, S.; Lin, V. *J. Am. Chem. Soc.* **2003**, *125*, 4451–4459.
(34) Tang, D.; Sauceda, J.; Lin, Z.; Ott, S.; Basova, E.; Goryacheva, I.; Biselli, S.; Lin, J.; Niessner, R.; Knopp, D. *Biosens. Bioelectron.* **2009**, *25*, 514–518.
(35) Su, B.; Tanng, J.; Chen, H.; Huang, J.; Chen, G.; Tang, D. *Anal. Methods* **2010**, *2*, 1702–1709.
(36) Suhren, G.; Knappstein, K. *Analyst* **1998**, *123*, 2797–2801.